Piezoelectric contributions to pulsed degenerate four-wave mixing

Ivan Biaggio[a)]
Institute of Quantum Electronics, Swiss Federal Institute of Technology, ETH Hönggerberg, CH-8093 Zürich, Switzerland

(Received 6 November 2000; accepted for publication 2 February 2001)

The existence of geometry and pulse-length-dependent piezoelectric contributions to pulsed degenerate four-wave mixing is demonstrated experimentally. These effects must be taken into account when measuring third-order susceptibilities in noncentrosymmetric materials. © *2001 American Institute of Physics.* [DOI: 10.1063/1.1358850]

In solid-state materials lacking a center of symmetry, cascaded second-order nonlinear optical effects,[1–3] especially the combination of optical rectification and the linear electro-optic effect, are an important contribution to degenerate four-wave mixing (DFWM),[4,5] an experimental tool widely used to measure the third-order nonlinear optical susceptibility. This quantity determines the magnitude of several interesting phenomena,[6] among which the optical Kerr effect, self-phase modulation, soliton formation, and the interaction of different optical waves, with applications like optical limiting and all-optical switching.

In order to extract an accurate value of the third-order susceptibility of noncentrosymmetric materials from a DFWM experiment, it is necessary to take into account the peculiar geometry dependences introduced by second-order effects.[4,5,7] They can both lead to misleading results, if ignored, or to alternative possibilities for calibrating DFWM experimental setups, if properly taken into account.[5] Some predicted effects of the electro-optic and optical rectification contributions to DFWM have been observed in Refs. 4, 5, and 7. This letter now reports the experimental observation of another, associated effect: the nanosecond fast piezoelectric relaxation whose contributions to DFWM were calculated in Ref. 5. This is important because the possibility of piezoelectric relaxation introduces additional dependencies of the DFWM signal from the angle between the interacting beams and from the pulse length. This must be taken into account in order to be able to compare experimental results obtained with different DFWM setups.

At the origin of the piezoelectric contributions discussed in this work are two space-modulated rectified polarizations induced by two pairs of interacting waves in DFWM. For the experimental configuration shown schematically in Fig. 1, the rectified polarizations can be described by two static (on the time scale of the pulse length used in DFWM) plane waves with wave vectors $\mathbf{k}_a$ and $\mathbf{k}_b$.[4,5] Approximating the interacting beams and the generated polarizations by plane waves with real amplitude $(1/2)\mathbf{A}(\omega,\mathbf{k})\exp[i(\omega t-\mathbf{k}\cdot\mathbf{x})]+\text{c.c.}$ and complex amplitude $\mathbf{A}(\omega,\mathbf{k})$, one can write the complex amplitude of the rectified polarization with wave vector $\mathbf{k}_a$ as

$$P_p^{(\mathrm{OR})}(\omega=0,\mathbf{k}_a)=\epsilon_0\chi_{pjl}^{(2)}(0,-\omega,\omega)\times E_j(-\omega,-\mathbf{k}_3)E_l(\omega,\mathbf{k}_1), \tag{1}$$

where ϵ_0 is the permittivity of vacuum, $E_n(\omega,\mathbf{k})$ is the component of the electric-field amplitude along n, $E_n(-\omega,-\mathbf{k})$ is its complex conjugate, and $\chi_{pjl}^{(2)}(0,-\omega,\omega)$ is the second-order susceptibility describing optical rectification and the linear electro-optic effect. It is related to the standard electro-optic coefficients r_{ijk} by $\chi_{kij}^{(2)}(0,-\omega,\omega)=-(1/2)n_i^2n_j^2r_{ijk}$, where n_i is the refractive index for light polarized along the i axis. An analogous expression gives the rectified polarization with wave vector $\mathbf{k}_b$.[5]

The electro-optic interaction of one of the input beams with these optical rectification gratings contributes to DFWM, and can be represented by two effective nonlinear optical susceptibility tensors, $\chi_{ijkl}^{\mathbf{k}_a}$ and $\chi_{ijkl}^{\mathbf{k}_b}$, which must be added to the genuine third-order susceptibility $\chi_{ijkl}^{(3)}$ to get an effective susceptibility tensor $\chi_{ijkl}^{(3),\mathrm{EFF}}$ that describes DFWM in noncentrosymmetric materials. More details about the nomenclature used here for these tensors can be found in Ref. 5. The results of Ref. 5 can be cast in the form:

$$\chi_{ijkl}^{\mathbf{k}_a}=\frac{1}{6}n_i^2n_j^2n_k^2n_l^2r_{ikq}r_{jlp}\left[\zeta_{qp}(\mathbf{k}_a)+\frac{\delta_{qp}}{\epsilon_{pp}+2}\right], \tag{2}$$

$$\chi_{ijkl}^{\mathbf{k}_b}=\frac{1}{6}n_i^2n_j^2n_k^2n_l^2r_{ilq}r_{jkp}\left[\zeta_{qp}(\mathbf{k}_b)+\frac{\delta_{qp}}{\epsilon_{pp}+2}\right], \tag{3}$$

where r_{ijk} and ϵ_{ij} are effective electro-optic and dielectric tensors to be discussed below, $\delta_{qp}=0, q\neq p; \delta_{qp}=1, q=p$, and $\zeta_{qp}(\mathbf{k})$ is

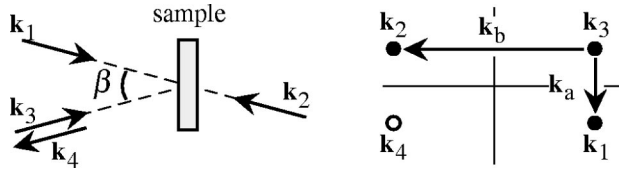

FIG. 1. DFWM geometry of interest. The experimental configuration with the interacting wave vectors is shown on the left, while the wave-vector coordinates are plotted on the right ($\mathbf{k}_4$, given by the white circle, is the wave vector of the signal beam). The plot also shows the wave vectors $\mathbf{k}_a$ and $\mathbf{k}_b$ of the optical rectification gratings that are responsible for the largest second-order contributions to DFWM. For clarity, the abscissa and ordinate axes are not in scale.

a)Electronic mail: biaggio@phys.ethz.ch

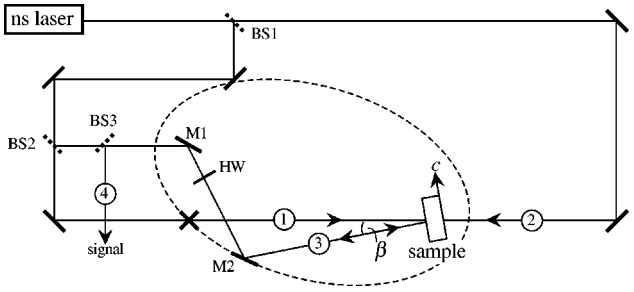

FIG. 2. DFWM experimental setup. The individual path lengths of the three input nanosecond pulses are the same. The path lengths of beams 1 and 2 are made equal by adjusting the sample position. The path length of beam 3 is fixed by moving mirror M2 on the ellipse (drawn dashed in the figure) which has its two foci at the positions of mirror M1 and the sample, and which intersects the path of beam 1 in the spot directly below mirror M1 (marked by a cross) where the path lengths of beams 1 and 3 are equal.

$$\zeta_{qp}(\mathbf{k}) = -\frac{k_q k_p}{k_k \epsilon_{kl} k_l}. \tag{4}$$

In Eqs. (2) and (3), ζ_{qp} can be substituted with $\zeta_{qp}=0$ for a transverse polarization (perpendicular to $\mathbf{k}$) and with $\zeta_{qp} = -\delta_{qp}/\epsilon_{pp}$ for a longitudinal polarization (parallel to $\mathbf{k}$) oriented along the p axis.

Piezoelectric effects become important when the propagation time of an acoustic elastic wave over a distance equal to the modulation period of the rectified polarization [$\Lambda = 2\pi/k_a$ for Eq. (1)] is shorter than the laser pulse length used. In this case a strain pattern can be established in the crystal while the interacting pulses are still present, and it leads to additional contributions to the DFWM signal. These additional contributions can be included in the limit of long wave vectors by using, in Eqs. (2)–(4), effective electro-optic and dielectric tensors that take into account that the crystal—because of the sinusoidal spatial modulation of the rectified polarizations—is neither in a completely strain-free case, nor in a completely stress-free case. These effective tensors can be calculated by[5]

$$r_{ijk}(\mathbf{k}) = r^S_{ijk} + p_{ijmn} e_{klu} \hat{\kappa}_n \hat{\kappa}_u (A^{-1})_{ml}, \tag{5}$$

$$\epsilon_{ij}(\mathbf{k}) = \epsilon^S_{ij} + \frac{1}{\epsilon_0} \hat{\kappa}_n \hat{\kappa}_k e_{imk} e_{jln} (A^{-1})_{ml}, \tag{6}$$

where $\mathbf{k}$ is the wave vector of the corresponding optical rectification grating [see Eq. (1)], r^S_{ijk} is the electro-optic tensor at constant strain, ϵ^S_{ij} is the dielectric tensor at constant strain, $\hat{\kappa}_i = k_i/k$, p_{ijkl} is the elasto-optic tensor, e_{ijk} is the piezoelectric tensor, $A_{ik} = C^E_{ijkl} \hat{\kappa}_j \hat{\kappa}_l$, and C^E_{ijkl} is the elastic stiffness tensor. For short wave vectors the crystal has no time to elastically relax, and $r_{ijk}(\mathbf{k}) = r^S_{ijk}$, $\epsilon_{ij}(\mathbf{k}) = \epsilon^S_{ij}$.

This leads to a dependence of the third-order susceptibility determined in DFWM on the length of the wave vector of the rectified polarization grating, a fact that influences DFWM measurements in various ways. As an example, in the arrangement of Fig. 1 the wave vector $\mathbf{k}_b$ is generally quite long, and piezoelectric relaxation can already become possible in some picoseconds. The $\mathbf{k}_b$ contribution will thus be different for experiments performed, e.g., with 100 ps pulses and for experiments performed with 1 ps pulses. However, to directly observe such an effect, one would need to tune the pulse length, which is impractical.

To experimentally demonstrate the existence of the piezoelectric contribution, and to relate its magnitude to the predicted theoretical value, it is better to focus on the rectified polarization grating with the shorter wave vector $\mathbf{k}_a$. When the duration of the laser pulse is similar to the acoustic wave propagation time discussed above, the effect of piezoelectric relaxation can be observed by using a nanosecond laser in the experimental configuration of Fig. 1 and measuring the DFWM signal as a function of the angle β between the interacting beams, which is related to the spatial period $\Lambda = 2\pi/k_a$ of the optical rectification grating by $\Lambda = \lambda/[2\sin(\beta/2)]$, with λ the laser wavelength in vacuum.

Barium titanate ($BaTiO_3$) is a good candidate to observe these effects because its electro-optic, piezoelectric, and elastic properties are well characterized, and because it has large electro-optic coefficients. All the relevant material parameters have been tabulated in Ref. 8 and the dispersion of the electro-optic coefficients is given in Ref. 9. $BaTiO_3$ has tetragonal symmetry with point group $mm4$, with the c axis parallel to the ferroelectric polarization. The piezoelectric contribution is expected to be particularly strong for $\chi^{\mathbf{k}_a \| c}_{1133}$, i.e., for the contribution of the optical rectification grating with wave vector $\mathbf{k}_a$ when the c axis of the crystal is parallel to $\mathbf{k}_a$. Numerical values are given below. They were all calculated using the material parameters in Refs. 8 and 9 at a wavelength of 1.06 μm.

The DFWM experiments were realized with a Q-switched laser producing 7-ns-long pulses at a wavelength of 1.064 μm and the experimental setup shown in Fig. 2. This setup has been especially constructed to allow a relatively easy adjustment of the angle between the beams while keeping the path lengths of all beams, and therefore, the relative coherence of the interacting pulses, constant. To measure the effective susceptibility $\chi^{(3),\mathrm{EFF}}_{1133}$, beams 1 and 2 were polarized in the plane of incidence, while beams 3 and 4 were polarized perpendicular to it (by the half-wave plate marked ''HW'' in Fig. 2).

For the $BaTiO_3$ crystal oriented as in Fig. 2, with its c axis in the beam incidence plane, $\chi^{\mathbf{k}_a \| c}_{1133}$ contributes to the signal, and it is proportional to $(r_{131})^2/(\epsilon_{11}+2)$ [see Eq. (2)]. It can be calculated to be $\chi^{\mathbf{k}_a \| c}_{1133} = (224 \pm 45) \times 10^{-22}\,\mathrm{m^2/V^2}$ when the strain-free tensor components are used.[5] When elastic relaxation is allowed, the effective electro-optic and dielectric coefficients of Eqs. (5) and (6) must be used, resulting in $\chi^{\mathbf{k}_a \| c}_{1133} = (355 \pm 70) \times 10^{-22}\,\mathrm{m^2/V^2}$. The errors are estimated on the basis of a $\sim$10% uncertainty in the dielectric and electro-optic tensors.[8] The inclusion of piezoelectric effects does not lead to larger uncertainties because—in this particular case in $BaTiO_3$—only a shear deformation can be induced, and the effective tensors calculated from Eqs. (5) and (6) correspond to the stress-free values, which can be taken directly from Ref. 9. The magnitude of the total piezoelectric contribution in this case is thus expected to be $(130 \pm 60) \times 10^{-22}\,\mathrm{m^2/V^2}$ (the error takes into account that this value is calculated from a difference, but also that any errors in the strain-free and stress-free values of the material tensors are not necessarily uncorrelated). The contribution from the rectification grating with wave vector $\mathbf{k}_b$ is fixed at $\chi^{\mathbf{k}_b \perp c}_{1133} = (224 \pm 45) \times 10^{-22}\,\mathrm{m^2/V^2}$ because there

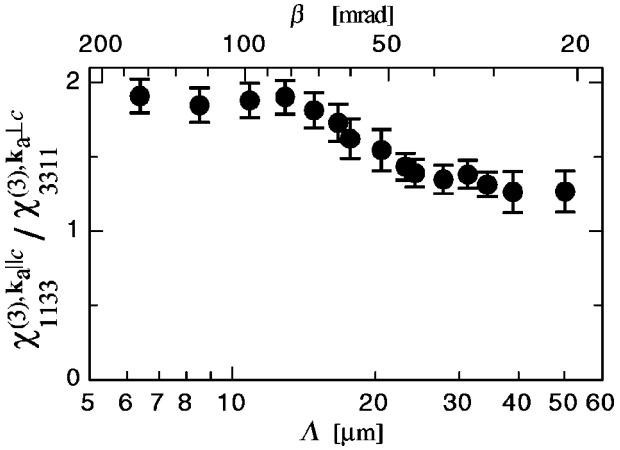

FIG. 3. Effective third-order susceptibility vs the angle β between the beams, or vs the spatial period Λ of the rectified polarization grating ($\Lambda = 2\pi/k_a = \lambda/[2\sin(\beta/2)]$).

any piezoelectric contribution vanishes by symmetry, as follows from Eq. (5). The experimental value of the effective DFWM third-order susceptibility should thus increase by approximately $(25\pm13)\%$ over its $(560\pm80)\times10^{-22}\,\mathrm{m^2/V^2}$ strain-free value[5] when the wave vector of the rectified polarization increases to a magnitude that allows for elastic relaxation during the pulse duration.

The beam intersection angle when this increase takes place is given by the modulation period $\Lambda = 2\pi/k_a$ of the rectified polarization grating for which the propagation time of a transverse acoustic wave is similar to the pulse duration of 7 ns. From the relevant speed of sound of a transverse wave, $v = \sqrt{C^E_{1313}/\rho} = 3.18\,\mu$m/ns ($\rho$ is the mass density), one gets $\Lambda \approx 20\,\mu$m. This corresponds to a beam intersection angle β between 50 and 60 mrad.

An important fact that can be exploited for the measurements is that when the $BaTiO_3$ crystal is oriented with its c axis perpendicular to the beam incidence plane, $\chi^{\mathbf{k}_a\perp c}_{3311}$ vanishes almost completely.[5] For this crystal orientation no dependence of the DFWM signal from the beam intersection angle β is expected. In addition, for both $c\|\mathbf{k}_a$ and $c\perp\mathbf{k}_a$, $\chi^{\mathbf{k}_b\perp c}_{1133}$ is the same and independent of the angle between the interacting beams.

It follows that the effects of possible variations of mirror reflectivity and/or beam overlap conditions when changing the beam intersection angle can be avoided by measuring the DFWM signal for both $c\|\mathbf{k}_a$ and $c\perp\mathbf{k}_a$ and taking the ratio between the two values. Because of the expected constancy of the signal for $c\perp\mathbf{k}_a$, the data measured in such a way should directly reflect the dependence of $\chi^{\mathbf{k}_a\|c}_{1133}$ on the magnitude of $\mathbf{k}_a$, or the beam intersection angle β.

The results are shown in Fig. 3. The data points are averages over several measurements. The effect of acoustic phonons for longer wave vectors can clearly be seen as the increase of the third-order susceptibility when the angle between the beams increases. The transition from a lower to a higher susceptibility value does indeed take place for a period of the rectified polarization grating around 20 μm, as expected from the estimation above. The ratio between the two susceptibility values at short and long wave vectors is higher than the value calculated above, but is within the expected uncertainties. The value of $\chi^{\mathbf{k}_a\|c}_{1133}/\chi^{\mathbf{k}_a\perp c}_{3311}$ measured at short wave vectors is somewhat lower than what is expected from the calculated values of the second-order contributions,[5] but this small discrepancy is also within the experimental error.

The piezoelectric effect whose signature is visible in Fig. 3 is peculiar to DFWM in noncentrosymmetric materials. In contrast to the example of thermal gratings, where—given short enough pulses—acoustic phonons can be induced and detected (as an oscillation of the signal intensity as a function of the delay time of the probe pulse) no matter what the magnitude of the wave vector $\mathbf{k}_a$ is, in the process observed here acoustic phonons only contribute to the signal if their characteristic frequency (given by the the speed of sound divided by the spatial period of the rectification grating) is higher than the frequency content of the laser pulses. Their effect can only be seen as a dependence of the DFWM signal from the pulse length, or from the angle between the beams.

It should be noted that in this experiment the beams inducing the rectified polarization gratings are always polarized perpendicular to each other, so that there is no light intensity modulation with wave vector $\mathbf{k}_a$ or $\mathbf{k}_b$. A generation of acoustic phonons by transient temperature gratings can, therefore, be excluded, together with any other effects relying on spatially inhomogeneous energy deposition.

In conclusion, the measurements presented above give a clear demonstration of the existence of piezoelectric contributions to pulsed DFWM, which must be taken into account in order to determine reliable values of third-order susceptibilities in noncentrosymmetric materials, and to be able to compare DFWM experiments performed with different pulse lengths or experimental setups.

[1] T. K. Gustafson, J.-P. E. Taran, P. L. Kelley, and R. Y. Chiao, Opt. Commun. **2**, 17 (1970).
[2] E. Yablonovitch, C. Flytzanis, and N. Blomebergen, Phys. Rev. Lett. **29**, 865 (1972).
[3] C. Flytzanis, in *Quantum Electronics*, edited by H. Rabin and C. L. Tang (Academic, New York, 1975), Vol. 1.
[4] M. Zgonik and P. Günter, J. Opt. Soc. Am. B **13**, 570 (1996).
[5] I. Biaggio, Phys. Rev. Lett. **82**, 193 (1999).
[6] R. W. Hellwarth, Prog. Quantum Electron. **5**, 1 (1977).
[7] Ch. Bosshard, I. Biaggio, St. Fischer, S. Follonier, and P. Günter, Opt. Lett. **24**, 196 (1999).
[8] M. Zgonik, P. Bernasconi, M. Duelli, R. Schlesser, P. Günter, M. H. Garret, D. Rytz, Y. Zhu, and X. Wu, Phys. Rev. B **50**, 5941 (1994).
[9] P. Bernasconi, M. Zgonik, and P. Günter, J. Appl. Phys. **78**, 2651 (1995).